Published in final edited form as:

Cell. 2016 December 01; 167(6): 1481–1494.e18. doi:10.1016/j.cell.2016.11.013.

Impaired amino acid transport at the blood brain barrier is a cause of autism spectrum disorder

Dora C. Tarlungeanu[1], **Elena Deliu**[1], **Christoph P. Dotter**[1], **Majdi Kara**[2], **Philipp Christoph Janiesch**[3], **Mariafrancesca Scalise**[4], **Michele Galluccio**[4], **Mateja Tesulov**[1], **Emanuela Morelli**[1], **Fatma Mujgan Sonmez**[5], **Kaya Bilguvar**[6,7], **Ryuichi Ohgaki**[8], **Yoshikatsu Kanai**[8], **Anide Johansen**[9], **Seham Esharif**[10], **Tawfeg Ben-Omran**[11], **Meral Topcu**[12], **Avner Schlessinger**[13], **Cesare Indiveri**[4], **Kent Duncan**[3], **Ahmet Okay Caglayan**[14,15], **Murat Gunel**[15], **Joseph G. Gleeson**[9], and **Gaia Novarino**[1,16,*]

[1]Institute of Science and Technology (IST) Austria, Klosterneuburg, Austria

[2]Department of Pediatrics, Tripoli Children's Hospital, Tripoli, Libya

[3]Center for Molecular Neurobiology (ZMNH), University Medical Center Hamburg-Eppendorf (UKE), Hamburg, Germany

[4]Department DiBEST, unit of Biochemistry & Molecular Biotechnology, University of Calabria, Arcavacata di Rende, Italy

[5]Association of Developmental Child Neurology, Ankara, Turkey

[6]Department of Genetics, Yale School of Medicine, New Haven, Connecticut, USA

[7]Yale Center for Genome Analysis, Yale School of Medicine, Orange, Connecticut, USA

[8]Department of Bio-system Pharmacology, Graduate School of Medicine, Osaka University

[9]Department of Neuroscience, UCSD, Investigator, Howard Hughes Medical Institute, Rady Children's Institute for Genomic Medicine, USA

[10]Department of Pediatrics, Tripoli Children's Hospital, Tripoli, Libya

[11]Clinical and Metabolic Genetics, Weill Cornell Medical College, Department of Pediatrics, Hamad Medical Corporation, Doha, Qatar

[12]Department of Pediatric Neurology, Hacettepe University Children's Hospital, Ankara, Turkey

[13]Department of Pharmacological Sciences, Icahn School of Medicine at Mount Sinai School of Medicine, New York, USA

[*]Correspondence to: gnovarino@ist.ac.at.

[16]Lead contact

AUTHOR CONTRIBUTIONS

D.C.T, E.D., C.D., M.T., E.M., A.J. G.N. performed experiments. G.N. conceived and supervised the study. M.K, F.M.S., K.B., S.E., T.BO., A.O.C., M.G., J.G.G. recruited and characterized patients. A.O.C., G.N., performed and analyzed WES. D.C.T., P.C.J., K.D., performed polysome experiments. M.S., M.G., C.I., performed protoliposome experiments. A.S., performed in silico analysis. R.O., Y.K., generated and tested LAT1 antibody. G.N. wrote the paper together with D.C.T, E.D, C.D. All authors read and approved the final version of the manuscript.

The authors declare no conflict of interests.

[14]Department of Medical Genetics, School of Medicine, Istanbul Bilim University, Istanbul, Turkey

[15]Departments of Neurosurgery, Genetics and Neurobiology, Program in Brain Tumor Research, Yale Program on Neurogenetics and Yale Comprehensive Cancer Center, Yale School of Medicine New Haven, Connecticut, USA

SUMMARY

Autism spectrum disorders (ASD) are a group of genetic disorders often overlapping with other neurological conditions. We previously described abnormalities in the branched chain amino acid (BCAA) catabolic pathway as a cause of ASD. Here we show that the *solute carrier transporter 7a5* (*SLC7A5*), a large neutral amino acid transporter localized at the blood brain barrier (BBB), has an essential role in maintaining normal levels of brain BCAAs. In mice, deletion of *Slc7a5* from the endothelial cells of the BBB leads to atypical brain amino acid profile, abnormal mRNA translation and severe neurological abnormalities. Furthermore, we identified several patients with autistic traits and motor delay carrying deleterious homozygous mutations in the *SLC7A5* gene. Finally, we demonstrate that BCAA intracerebroventricular administration ameliorates abnormal behaviors in adult mutant mice. Our data elucidate a neurological syndrome defined by *SLC7A5* mutations and support an essential role for the BCAA in human brain function.

INTRODUCTION

Autism spectrum disorders (ASD) is a group of syndromes of heterogeneous etiologies characterized by impairment in social interactions, verbal communication and repetitive behaviors. A number of twin and family studies have shown that genetics play a significant role in the development of ASD (Bailey et al., 1995; Folstein and Rutter, 1977). However, the genetic architecture of ASD is very complex and mutations in a single gene rarely account for a significant proportion of ASD patients. Despite their genetic heterogeneity, ASD may be less diverse functionally. Indeed, in many instances the great number of genes implicated in neurological disorders converges on a smaller number of biological pathways (De Rubeis et al., 2014).

We recently identified mutations in the gene *branched chain keto-acid dehydrogenase kinase* (*BCKDK*) in several patients with ASD, ID and epilepsy (Novarino et al., 2012). *BCKDK* is the enzyme responsible for the rate-limiting step in the catabolic pathway of the Branched Chain Amino Acids (BCAAs), a group of essential amino acids comprising valine, leucine and isoleucine. The most direct consequence of *BCKDK* mutations is a hyper-catabolism of the BCAAs, resulting in abnormally low levels of serum and brain BCAAs (Novarino et al., 2012).

The brain is dependent on a constant supply of BCAAs from the periphery. Should BCAAs be substantially important for the brain, factors facilitating BCAA uptake might be critical for the proper function of the central nervous system. The Large Neutral Amino Acid Transporter 1 (LAT1) is encoded by the *SLC7A5* gene (Verrey, 2003). The transporter is localized at the blood brain barrier (BBB) and forms a heterodimer with the glycoprotein CD98, encoded by the *SLC3A2* gene.

Here we studied a mouse model in which *Slc7a5* was deleted from the BBB and found that *Slc7a5* is particularly important to set brain BCAA levels within a normal range. Mice with defective BCAA transport at the BBB show abnormal activation of the amino acid response (AAR) pathway and a corresponding reduction in mRNA translation along with neuronal activity imbalance and behavioral problems. To probe whether *SLC7A5* is essential also in humans, we performed genetic analysis of a cohort of neurological pediatric patients. We identified and functionally validated, mutations in *SLC7A5* in several patients with ASD and motor coordination problems. Notably, neurological abnormalities can be treated in adult mice by 3-week long intracerebroventricular (i.c.v.) BCAA delivery.

RESULTS

SLC7A5 mediates BCAA flux at the BBB

Earlier *in vitro* studies described the sodium independent LAT1 as a large neutral amino acid (LNAA) transporter, including the BCAAs (Mastroberardino et al., 1998). The light subunit of the carrier, encoded by *SLC7A5*, is sufficient to transport LNAAs (Napolitano et al., 2015). The contribution of *SLC7A5* to brain LNAA/BCAA homeostasis *in vivo*, however, remains completely unknown.

To understand the physiological role of *Slc7a5 in vivo*, we employed a conditional (floxed) *Slc7a5* knock out mouse line (*Slc7a5*^{fl}) (Sinclair et al., 2013). In wild type animals, *Slc7a5* is considerably expressed in the plasma membrane of the endothelial cells of the BBB during development and in adulthood but it is mostly undetectable in other tissues (Figure 1A and Figure S1A–C). Thus, we crossed the *Slc7a5*^{fl} mouse with the *Tie2Cre* mouse line, expressing the Cre recombinase starting from embryonic day (E) 11.5 in the endothelial cells of blood vessels and BBB (Figure S1D) (Kisanuki et al., 2001). As expected, endothelial cells of the BBB of *Tie2*^{Cre}*;Slc7a5*$^{fl/fl}$ mice show complete lack of expression of *Slc7a5* (Figure 1A).

The exchange between blood and cerebrospinal fluid of a wide range of metabolically important molecules, including amino acids, is known to be constrained already early during development, arising with the BBB formation. However, some studies reported that many amino acids, including the BCAAs, are transported into the developing brain at much higher rate than in adulthood (Braun et al., 1980; Lefauconnier and Trouve, 1983). Whether this reflects a greater metabolic demand of the developing brain or the immaturity of the BBB is unknown (Watson et al., 2006). Hence, we asked how removal of *Slc7a5* from the BBB affects brain amino acid levels at different developmental stages.

We found that E14.5 *Tie2*^{Cre}*;Slc7a5*$^{fl/fl}$ mice don't show major changes in brain LNAA and BCAA levels (Figure 1B), suggesting either that at E14.5 the BBB is still immature, with amino acids leaking into the brain, or that another transporter may regulate LNAA and BCAA fluxes across the BBB during early development. In contrast, after birth and in adult stages brain BCAA, especially leucine and isoleucine, levels are abnormally low in *Tie2*^{Cre}*;Slc7a5*$^{fl/fl}$ animals (Figure 1C–D), indicating that *Slc7a5* expression is essential to regulate BCAA uptake by the brain. Surprisingly, the brain levels of several other LNAAs (e.g. tyrosine and tryptophan) in *Slc7a5* mutants are comparable to the ranges observed in

control (*Tie2*^{Cre}*;Slc7a5*$^{fl/+}$) animals, while a few other amino acids (e.g. histidine, serine and phenylalanine) show an elevated level in mutants compared to controls. In particular, brain histidine concentration is several fold higher in the *Tie2*^{Cre}*;Slc7a5*$^{fl/fl}$ mice than in control animals (Figure 1B–D). This result supports the idea that SLC7A5 works as an antiporter and that histidine is the main counter amino acid (Figure S2) (Napolitano et al., 2015).

Thus, in the absence of *Slc7a5* expression at the BBB, the mammalian brain accumulates histidine while failing to gather normal amounts of BCAAs. Importantly, neither the serum amino acid profile nor the level of brain neurotransmitters are affected in the *Tie2*^{Cre}*;Slc7a5*$^{fl/fl}$ animals (Figure S2C and Table S1). While this last result contradicts previous hypotheses (del Amo et al., 2008), it is in agreement with our in vitro experiments showing that SLC7A5 does not facilitate the movement of neurotransmitters (Figure S2A–B).

Deletion of *Slc7a5* from the BBB activates the AAR signal transduction pathway in the brain

In vitro, SLC7A5 transports not only the BCAAs but also other LNAAs, including phenylalanine, tyrosine and tryptophan (Napolitano et al., 2015). However, brain levels of these amino acids were not reduced in *Tie2*^{Cre}*;Slc7a5*$^{fl/fl}$ mice but rather slightly increased (Figure 1D). This suggests that additional BBB-located transporters might efficiently compensate for *Slc7a5* loss by mediating the passage of several LNAAs, but not of BCAAs. Indeed, RNA sequencing of mouse brain revealed a significant up-regulation of *Slc7a1* and *Slc7a3* genes (Figure 2A–B) encoding for the amino acid transporters Cat1 and Cat3 (Fotiadis et al., 2013). This finding suggests that *in vivo* Cat1 and Cat3 may contribute to preserve brain levels of LNAAs, other than BCAAs, in the *Tie2*^{Cre}*;Slc7a5*$^{fl/fl}$ mice.

Furthermore, differential gene expression analysis revealed the up-regulation of genes implicated in serine biosynthesis in *Tie2*^{Cre}*;Slc7a5*$^{fl/fl}$ mice (Figure 2B), explaining the modest but significant increase in brain serine level observed in the mutant animals (Figure 1D). An increase in the expression of genes encoding for amino acid transporters and serine biosynthetic enzymes has been previously linked to the activation of the AAR, a process implemented by individual cells to respond to amino acid deprivation (Kilberg et al., 2009). Consistently, RNAseq analysis of *Tie2*^{Cre}*;Slc7a5*$^{fl/fl}$ mouse brain, revealed the up-regulation of a number of other amino acid-related genes (e.g. aminoacyl-tRNA synthetases) (Figure 2A–B). Among them we noticed a significant up-regulation of mRNAs encoding for the amino acid responsive transcription factors *Atf4* and *Atf5* and the eukaryotic initiation factor 4E binding protein *4ebp1* (Figure 2A), all part of the AAR pathway. *Atf4* and *Atf5* have been implicated in the regulation of the central nervous system development and function. Specifically, *Atf4* modulates synaptic plasticity and long-term memory formation (Chen et al., 2003), while *Atf5* has been implicated in cell growth and development, especially in the nervous system (Angelastro et al., 2003). Aberrant expression of *Atf4* and/or *Atf5* has been implicated in cognitive dysfunctions and neuropsychiatric abnormalities, including altered emotional behavior (Green et al., 2008) and behavioral inflexibility (Trinh et al., 2012).

Importantly, our gene expression analysis didn't reveal any abnormality ascribable to increased histidine levels, suggesting that, despite histidine being the most affected amino

acid by *Slc7a5* deletion, changes in its level do not lead to severe molecular defects. Similarly, we didn't detect changes attributable to alterations of other amino acids such as phenylalanine.

Altered mRNA translation in *Slc7a5* mutant mice

Amino acid deprivation and activated AAR signaling pathway are associated with suppression of protein synthesis via phosphorylation of the translation initiation factor eIF2α. In the past few years several genes regulating mRNA translation have been implicated in cognitive deficits (Costa-Mattioli et al., 2005; Gkogkas et al., 2013; Santini et al., 2013). We therefore examined the effect of *Slc7a5* knock out at the BBB on translation and associated pathways in the brain.

To assess the impact of leucine and isoleucine deficiency on mRNA translation in the brain of $Tie2^{Cre};Slc7a5^{fl/fl}$ mice, we first performed western blot analysis of neocortical lysates obtained from wild-type and mutant animals. Specifically, we evaluated the expression and activity status of a number of proteins involved in the regulation of protein synthesis (Figure 2C). We observed a significant increase in the total levels of 4EBP1 protein (Figure 2C), consistent with increased 4EBP1 mRNA levels seen in our RNAseq data (Figure 2A), and of phosphorylated eukaryotic initiation factor 2 alpha (eIF2α) (Figure 2C), indicating that removal of *Slc7a5* from the BBB and the consequent decrease in brain BCAA concentration may lead to the suppression of cap-dependent translation initiation. In contrast, in none of our experiments did we detect abnormal activation of the mammalian target of rapamacyin (mTOR) pathway (Figure 2C), whose activity was shown to be regulated by leucine levels *in vitro* (Wolfson et al., 2016). This may suggest that *in vivo*, under chronic leucine deficiency, the mTOR complex is alternatively regulated.

To test whether abnormal regulation of 4EBP1 and eIF2α in mice lacking *Slc7a5* leads to changes in translation efficiency in the brain, we performed polysome profiling of wild type and $Tie2^{Cre};Slc7a5^{fl/fl}$ cortices. Importantly, in $Tie2^{Cre};Slc7a5^{fl/fl}$ mouse cortical lysates we observed a significant shift of ribosomes from actively translating polysomes toward the monosomal fraction (Figure 2D), the hallmark of decreased translation initiation. We conclude that BCAA shortage and associated effects of 4EBP1 levels and increased eIF2α phosphorylation elicit deficient translation initiation in the brain.

Slc7a5 conditional knock out animals show motor delay and autism-related phenotypes

Behavioral impairments resulting from abnormal regulation of cap-dependent translation have been previously described (Banko and Klann, 2008; Santini et al., 2013; Trinh et al., 2012). Thus, we tested $Tie2^{Cre};Slc7a5^{fl/fl}$ mice for global behavioral changes. $Tie2^{Cre};Slc7a5^{fl/fl}$ mice are born at Mendelian ratio and appear normal in size but display kyphosis (44% of mutant mice) and hind limb clasping (89% of mutant mice). In an open field $Tie2^{Cre};Slc7a5^{fl/fl}$ mice show reduced explorative behavior and lower velocity (Figure 3A). Rearing, a form of vertical exploration, was significantly reduced in the $Tie2^{Cre};Slc7a5^{fl/fl}$ mice (Figure 3B). Nonetheless, *Slc7a5* mutant mice and wild type littermates have similar habituation time course (Figure S3A), suggesting that the diminished activity results from locomotion defects rather than a faster habituation to the

field. Therefore we tested the *Tie2*^{Cre}*;Slc7a5*$^{fl/fl}$ mice for fine motor coordination and locomotion problems. Indeed, *Tie2*^{Cre}*;Slc7a5*$^{fl/fl}$ animals presented significant difficulties in the walking beam test (Figure 3C) and gait abnormalities (Figure 3D–E).

Since in our previous work we implicated BCAA deficiency in ASD (Novarino et al., 2012), we tested *Tie2*^{Cre}*;Slc7a5*$^{fl/fl}$ for autism-like phenotypes. *Tie2*^{Cre}*;Slc7a5*$^{fl/fl}$ do not show excessive grooming or perseverative behaviors (Figure S3B), activities which can be, however, severely complicated by the presence of motor deficits in the mutants. Thus, we tested *Tie2*^{Cre}*;Slc7a5*$^{fl/fl}$ mice for social interaction abnormalities. We first employed a three-chamber social arena to probe the mutant animals for self-initiated interactions with a wild-type unfamiliar mouse. This analysis revealed that while wild-type mice have more close interactions with an unfamiliar mouse than an object, the *Tie2*^{Cre}*;Slc7a5*$^{fl/fl}$ mice show no preference between these two (Figure 3F). We then tested juvenile animals for social play and found that *Tie2*^{Cre}*;Slc7a5*$^{fl/fl}$ mice tend to stay farther apart from their cage-mate and display a decreased number of nose-to-nose contacts (Figure 3G). Finally, we measured isolation-induced ultrasonic vocalizations (USV) emitted by mouse pups separated from the mother. *Tie2*^{Cre}*;Slc7a5*$^{fl/fl}$ pups display increased number of USV starting from P8 when compared with their wild-type littermates (Figure 3H), a behavior observed in other autism models (Gkogkas et al., 2013). Interestingly, the excessive number of USVs emitted by the mutant pups may be due to an increased repetition of a specific repertoire of vocalization patterns (Romano et al., 2013).

Inhibitory activity defects in *Tie2*^{Cre}*;Slc7a5*$^{fl/fl}$ mice

Social interaction abnormalities have been suggested to arise from cortical excitation/inhibition imbalance (Yizhar et al., 2011), a correlation also observed in animals with abnormal regulation of translation (Gkogkas et al., 2013; Santini et al., 2013). We evaluated synaptic function in 21 days old *Tie2*^{Cre}*;Slc7a5*$^{fl/fl}$ mice using whole-cell recordings of pyramidal neurons in layer 2/3 of the somatosensory cortex. Examination of synaptic transmission revealed a slight increase in the amplitude of miniature excitatory postsynaptic currents (mEPSCs) and a marked reduction in the frequency of miniature inhibitory synaptic currents (mIPSCs) (Figure 4A–B), indicating a significant excitation/inhibition imbalance.

To determine whether the synaptic alterations in *Tie2*^{Cre}*;Slc7a5*$^{fl/fl}$ mice are selective to the somatosensory cortex, we performed the same experiment in other brain regions. Given the locomotion abnormalities observed in *Tie2*^{Cre}*;Slc7a5*$^{fl/fl}$ mice, we tested inputs received by the Purkinje cells. Similarly to the neocortex, *Tie2*^{Cre}*;Slc7a5*$^{fl/fl}$ mouse cerebellar Purkinje cells display a significant reduction in mIPSC frequency (Figure S3C–D).

Changes in mIPSC frequency are generally due to differences in the number of functional synaptic sites and/or in the presynaptic release probability at existing sites (changes in the GABA vesicular pool or vesicular turnover rate). Therefore, we examined overall brain morphology (Figure S4A), cortical layering (Figure S4B) and inhibitory neuron distribution (Figure S4C) and found that for these parameters somatosensory cortices of mutant animals were undistinguishable from the control. We further looked for differences in pre- and postsynaptic markers of inhibitory synapses. Importantly, we observed that the intensity of the vesicular GABA transporter (VGAT) staining, a marker for GABAergic presynaptic

terminals, was lower in the somatosensory cortices of *Tie2*^{Cre}*;Slc7a5*$^{fl/fl}$ mice (Figure 4C and Figure S4D). However, the GABAergic postsynaptic marker neuroligin 2 (Varoqueaux et al., 2004) appeared qualitatively and quantitatively similar in the somatosensory cortex of the mutant and control mice (Figure 4D and Figure S4E). The marked reduction of VGAT and normal neuroligin 2 protein levels in *Tie2*^{Cre}*;Slc7a5*$^{fl/fl}$ mice were also confirmed by western blot analysis of cortical lysates (Figure 4E). To determine whether the reduction in VGAT staining intensity was due to a specific lessening of VGAT or a decline in the number of VGAT-containing vesicles we analyzed inhibitory synapses by electron microscopy. In agreement with the electrophysiology results, we detected a significant reduction of vesicle number in symmetric synapses in the somatosensory cortices of *Tie2*^{Cre}*;Slc7a5*$^{fl/fl}$ mice compared with control animals (Figure 4F).

Tie2^{Cre}*;Slc7a5*$^{fl/fl}$ mutant mice resemble *Bckdk* knock out animals

The reduction in brain BCAA levels observed in *Tie2*^{Cre}*;Slc7a5*$^{fl/fl}$ adult mice is comparable to what we measured in *Bckdk*$^{-/-}$ animals (Novarino et al., 2012). *Bckdk*$^{-/-}$ mice, in addition, display reduced serum BCAA levels and a marked increase in brain levels of several other LNAAs (Novarino et al., 2012) but normal neurotransmitter concentrations (Figure S5G). Thus, it remained unclear whether neurological abnormalities in *BCKDK* mutant patients and mice are due to alterations in serum or brain BCAA. Alternatively, the pathological conditions observed in patients carrying mutations in *BCKDK* could be due to increased brain LNAA levels.

We compared *Bckdk*$^{-/-}$ and *Tie2*^{Cre}*;Slc7a5*$^{fl/fl}$ mouse lines and observed a great phenotypic overlap. Similarly to *Tie2*^{Cre}*;Slc7a5*$^{fl/fl}$ mice, *Bckdk* mutants show motor coordination abnormalities, autism-related behaviors, decreased mIPSC frequency (Figure S5A–F) and activation of the AAR pathway (Novarino et al., 2012) implying that *Bckdk*$^{-/-}$ and *Tie2*^{Cre}*;Slc7a5*$^{fl/fl}$ mice share pathophysiological mechanisms.

SLC7A5 mutations in patients with ASD and motor delay

Given the essential role of *SLC7A5* in regulating brain BCAA homeostasis and the phenotypic overlap between *Bckdk* and *Slc7a5* mutant mice, we reasoned that mutations in *SLC7A5*, could lead to ASD and motor abnormalities in humans. Thus, we collaboratively screened whole exome sequencing (WES) data from more than 2000 families with documented parental consanguinity, presenting with children with various neurological diseases. We identified two independent families with multiple children affected by ASD, microcephaly and motor problems all harboring homozygous missense mutations in the gene *SLC7A5*.

Family 1426 is a consanguineous family with two branches and 5 affected individuals (Figure 5A–C). WES analysis of patients 1426-5 and 1426-19 (Figure 5A) identified a unique shared homozygous missense variant in the *SLC7A5* gene (Table S2). The homozygous mutation falls in a linkage pick with LOD score >4 (Figure S6A) and segregates with the disorder in the rest of the family (confirmed by Sanger sequencing). The A246V mutation changes a highly conserved alanine situated in a stretch of preserved amino acids predicted to be important for amino acid transport (Figure 6A–B). In an additional

cohort of 1000 neurodevelopmental disorder patients analyzed by WES we identified Family 1465 including two patients with identical ASD, microcephaly and motor delay (Figure 5A–C) sharing a predicted deleterious homozygous mutation (Figure S6B) in *SLC7A5* leading to the change of the conserved proline in position 375 to a leucine (P375L) (Figure 6A). Both genetic variants were not present in more than 200 ethnically-matched, healthy control chromosomes, nor in our data set of over 2000 chromosomes or in publicly available databases (Table S2).

Functional assessment of *SLC7A5* A246V and P375L mutations

We mapped the two genetic variants onto a homology model of SLC7A5 (Geier et al., 2013). A246 is located in transmembrane helix 6 in close proximity to the extracellular side and to the channel (Figure 6B). Mutation of this residue to the larger valine is therefore likely to impact the transporter's structure by disrupting helix–helix packing and ligand transport. P375 is located in transmembrane helix 9 in close proximity to the cytoplasmic side (Figure 6B). Proline often plays a key role in introducing kinks in helices and allowing conformational changes important for transporter function. Thus, mutation of this residue to leucine is likely to disrupt the flexibility required for transport by SLC7A5.

To validate the functional impact of the A246V and P375L substitution we performed transport assays. Therefore, the recombinant A246V and P375L mutant proteins were successfully expressed (Figure S7A), reconstituted in proteoliposomes (Figure 6C–D) and tested with a series of transport assays (Napolitano et al., 2015).

From transport time course analysis it was evident that the mutant A246V was virtually inactive (Figure 6C). As predicted by the homology model (Figure 6B) the functional defect may be ascribed to a higher steric hindrance of the valine side chain with respect to that of alanine. To verify this hypothesis and that the functional change was specifically ascribed to the pathological variant we analyzed an artificial mutant, A246G, (Figure S7A) in which the 246 side chain had been abolished. In contrast to the patient-specific A246V mutation, the A246G variant didn’t show any transport defect (Figure 6C and Figure S7B). To exclude that the loss of activity observed in the A246V mutant could be due to reconstitution failing, we assessed the efficiency of protein reconstitution. We found no differences in the reconstitution of the A246V mutant compared to the WT protein (Figure S7A). Taken together, all the data confirmed that the substitution of A246V was functionally disruptive.

In contrast, the P375L mutant showed no significant variations in time dependent activity and external Km with respect to WT (Figure S7C–D). Owing to the location of P375 in an intracellular moiety of the protein (Figure 6B), we determined also the internal Km for this mutant (about 25 mM; 27 ± 9.9) (Figure S7E). Interestingly, the Km value was roughly five times that of the WT (about 5 mM; 5.2 ± 2.3), suggesting that some variations in the substrate binding/translocation pathway may occur upon mutation. We further performed efflux experiments for evaluating possible differences in the antiport reaction catalyzed by SLC7A5. The measurements were performed using intraliposomal histidine concentration (2 mM), to create conditions similar to the intracellular environment. Surprisingly, the mutant P375L was mostly uncoupled. Indeed, while WT showed a very slow efflux in absence of external substrate, according to its antiport mode, the mutant unidirectional efflux was much

faster with a nearly complete proteoliposome emptying (Figure 6D). The anomaly observed in the P375L mutant indicates that, *in vivo*, loss of intracellular SLC7A5 substrate(s) impairs the driving force for taking up SLC7A5 substrates.

To further validate the functional impact of *SLC7A5* mutation in the patient-specific genetic background, we obtained human dermal fibroblasts from two affected and a few unaffected members of Family 1426 and Family 1465 and performed [^{3}H]-leucine uptake assay (Sinclair et al., 2013). *SLC7A5* transcript is expressed in human dermal fibroblasts and its level is not affected by the missense mutations (Figure S7F). Cells carrying the homozygous A246V or P375L variant, however, show a significant reduction in [^{3}H]-leucine uptake when compared with control cells (Figure 6E). Thus, the substitution of the SLC7A5 alanine 246 into a valine, or of the proline 375 into a leucine, is sufficient to significantly reduce the SLC7A5-mediated BCAA uptake.

BCAA intracerebroventricular injections rescue neurological abnormalities in adult *Slc7a5* mutant mice

The identification of ASD patients carrying mutations in the *SLC7A5* gene prompted the question whether this condition is potentially treatable. Therefore, we injected leucine and isoleucine stereotaxically into the brain of adult *Tie2*^{Cre}*;Slc7a5*$^{fl/fl}$ mice for 3 weeks (Figure 7A). Injected mice were then tested for some of the behavioral phenotypes described in Figure 3 and brain amino acid levels. Notably, after 3 weeks of i.c.v. leucine and isoleucine delivery (Figure 7A) their brain level was normalized (Figure 7B and Table S3) and the mutant mice showed a significant improvement in neurobehavioral abnormalities. Specifically, we observed a decreased number of *Tie2*^{Cre}*;Slc7a5*$^{fl/fl}$ mice showing the clasping (50% of injected vs 89% of non injected mutant mice) and the kyphosis phenotype (25% of injected vs 44% of non injected mutant mice). Most importantly, we could not detect any difference between treated *Tie2*^{Cre}*;Slc7a5*$^{fl/fl}$ and wild type mice in the open field test neither in velocity and distance moved nor in the number of rearings (Figure 7C). The gait of the injected *Tie2*^{Cre}*;Slc7a5*$^{fl/fl}$ mice was improved with a complete normalization of the sway length (Figure 7D). Importantly, wild type animals injected with the leucine/isoleucine mixture were indistinguishable from the non-injected animals of the corresponding genotype (Figure 7C–D), indicating that leucine and isoleucine specifically improve behavior of *Slc7a5* mutants. Worth mentioning is the fact that the rescue of the social and vocalization abnormalities could not be tested given technical issues presented by the presence of the implanted pump and the size of the animals (see STAR methods).

Although further tests are required to determine the extent and efficacy of the treatment, our data suggest that certain neurobehavioral abnormalities observed in *Slc7a5* mutants can be rescued by i.c.v. administration of leucine and isoleucine in adulthood. Even if we cannot entirely disregard a role of the increased level of other amino acids, these results support the idea that the reduction in brain leucine and isoleucine levels is the determinant factor in the appearance of the neurological phenotypes observed in humans and mice lacking *SLC7A5* expression.

DISCUSSION

Although SLC7A5 has been described as a BBB amino acid transporter, studies accurately verifying its expression or examining its function at the BBB are completely missing in the literature. Moreover, transport studies were performed using only *in vitro* systems thus lacking the expression of other carriers with possibly overlapping substrates and its physiological importance remained almost completely undetermined.

Our study shows that *SLC7A5* loss of function leads to ASD and motor dysfunctions in humans and mice. This fits with our previous work in which we have shown that mutations implicated in abnormal BCAA catabolism lead to ASD and fine motor coordination problems (Novarino et al., 2012). Along the same line, an increase in the brain levels of these same amino acids leads to the maple syrup urine disorder, characterized by cognitive dysfunctions, seizures and hypotonia (Menkes et al., 1954; Snyderman et al., 1964; Zinnanti et al., 2009). Although we acknowledge that ASD due to *SLC7A5* mutations may be an extremely rare condition, the present study indicates that fine-tuning of brain BCAA and LNAA concentrations is key for normal brain function and that mutations affecting genes contributing to BCAA homeostasis and the downstream signaling cascade may underlie a larger subgroup of ASD. In addition, this work has several important pathophysiological implications.

We show that *Slc7a5* expression at the BBB is particularly important to set a correct brain BCAA concentration. In fact, a lack of *Slc7a5* expression at the BBB leads to a significant reduction in brain BCAA levels, particularly leucine and isoleucine. Surprisingly, we didn't detect significant reductions in the brain levels of the other LNAAs, which in the mutant mice are rather slightly increased, indicating that additional carriers are involved in their transport. Among the most altered amino acids, beside leucine and isoleucine, we detected histidine, suggesting that this amino acid may have a special role in the function of the transporter. Noteworthy, the normal brain histamine levels (Figure S2C) as well as the RNAseq data obtained from mutant mice exclude an alteration of histaminergic transmission. Moreover, abnormally high serum and cerebrospinal fluid histidine levels have been reported in healthy individuals implying that increased histidine concentration is non-pathological (Lam et al., 1996).

Furthermore, we show that deletion of *Slc7a5* from the BBB leads to activation of the AAR pathway and reduced cap-dependent translation. How exactly abnormal regulation of translation leads to the observed phenotypes in *SLC7A5* mutant humans and mice remains to be investigated. However, we observed that inhibitory neurons may be more sensitive to altered amino acid levels as Atf5, a key molecule in the AAR pathway, has been reported to be preferentially expressed in GABA-synthetizing neurons (Zeisel et al., 2015). Accordingly, we found that deletion of *Slc7a5* from the BBB is sufficient to reduce cortical inhibitory activity, resulting in cortical excitation/inhibition imbalance and probably causing the observed neurological complications. Similarly, most of the functionally characterized ASD-mutations lead to an imbalance in the excitation/inhibition ratio. Thus, drugs acting on GABA transmission are considered an opportunity for the treatment of ASD and epilepsy (Braat and Kooy, 2015). It is therefore tempting to reason that identifying the rules by which

simple molecule such as the BCAAs may regulate GABAergic transmission might have a crucial impact on the development of novel therapeutic strategies for ASD.

Notably, besides representing a new subgroup of ASD, BCAA-related ASD may also represent a group of treatable conditions. Indeed, BCAA dietary administration in *BCKDK* null mice and humans (Novarino et al., 2012), as well as leucine and isoleucine i.c.v. injection in adult $Tie2^{Cre};Slc7a5^{fl/fl}$ mice lead to a significant improvement of the neurobehavioral abnormalities.

STAR ★ METHODS

Detailed methods are provided in the online version of this paper and include the following:

- KEY RESOURCES TABLE
- CONTACT FOR REAGENT AND RESOURCE SHARING
- EXPERIMENTAL MODEL AND SUBJECT DETAILS
  - Mice
  - Human subjects and sample collection
  - Cell lines
  - Protein model
- METHOD DETAILS
  - Amino acid analysis
  - RNA-sequencing
  - Western blot
  - Polysome profiling
  - Immunohistochemistry
  - Nissl staining
  - Electrophisiology
  - Electron microscopy
  - Behavioral studies
  - Intracerebroventricular dye injection
  - Serial surgical implantation of cannula and osmotic pumps
  - Whole exome sequencing, homozygosity profile and variant prioritization
  - Sanger sequencing
  - Leucine uptake assay

- Cloning, mutagenesis and expression of the human SLC7A5 wild-type and mutants
- Purification of human SLC7A5 wild-type and mutants
- Reconstitution of human SLC7A5 wild-type and mutants in proteoliposomes
- Transport measurements
- Ultracentrifugation of proteoliposomes

- QUANTIFICATION AND STATISTICAL ANALYSIS
  - Amino acid data
  - RNA-sequencing
  - Protein data
  - Imunohistochemistry
  - Neuronal data
  - Electron microscopy
  - Behavior
  - Transport measurement data
- DATA AND SOFTWARE AVAILABILITY
  - Data resources

Supplementary Material

Refer to Web version on PubMed Central for supplementary material.

Acknowledgments

We thank A.C. Manzano and F. Marr for technical assistance, R. Shigemoto and the IST Austria Electron Microscopy (EM) Facility for assistance. We acknowledge support from CIDR for genome wide SNP analysis (X01HG008823) and Broad Institute Center for Mendelian Disorders (UM1HG008900 to D. MacArthur), the Yale Center for Mendelian Disorders (U54HG006504 to M.G.), the Gregory M. Kiez and Mehmet Kutman Foundation (M.G.), Italian Ministry of Instruction University and Research (PON01_00937 to C.I.), NIH (R01-GM108911 to A.S.). This work was supported by NICHD (P01HD070494), SFARI (grant 275275) to J.G.G and FWF (SFB35_3523) to G.N.

References

Angelastro JM, Ignatova TN, Kukekov VG, Steindler DA, Stengren GB, Mendelsohn C, Greene LA. Regulated expression of ATF5 is required for the progression of neural progenitor cells to neurons. The Journal of neuroscience : the official journal of the Society for Neuroscience. 2003; 23:4590–4600. [PubMed: 12805299]

Bailey A, Le Couteur A, Gottesman I, Bolton P, Simonoff E, Yuzda E, Rutter M. Autism as a strongly genetic disorder: evidence from a British twin study. Psychol Med. 1995; 25:63–77. [PubMed: 7792363]

Banko JL, Klann E. Cap-dependent translation initiation and memory. Progress in brain research. 2008; 169:59–80. [PubMed: 18394468]

Braat S, Kooy RF. The GABAA Receptor as a Therapeutic Target for Neurodevelopmental Disorders. Neuron. 2015; 86:1119–1130. [PubMed: 26050032]

Braun LD, Cornford EM, Oldendorf WH. Newborn rabbit blood-brain barrier is selectively permeable and differs substantially from the adult. Journal of neurochemistry. 1980; 34:147–152. [PubMed: 7452231]

Chen A, Muzzio IA, Malleret G, Bartsch D, Verbitsky M, Pavlidis P, Yonan AL, Vronskaya S, Grody MB, Cepeda I, et al. Inducible enhancement of memory storage and synaptic plasticity in transgenic mice expressing an inhibitor of ATF4 (CREB-2) and C/EBP proteins. Neuron. 2003; 39:655–669. [PubMed: 12925279]

Costa-Mattioli M, Gobert D, Harding H, Herdy B, Azzi M, Bruno M, Bidinosti M, Ben Mamou C, Marcinkiewicz E, Yoshida M, et al. Translational control of hippocampal synaptic plasticity and memory by the eIF2alpha kinase GCN2. Nature. 2005; 436:1166–1173. [PubMed: 16121183]

De Rubeis S, He X, Goldberg AP, Poultney CS, Samocha K, Cicek AE, Kou Y, Liu L, Fromer M, Walker S, et al. Synaptic, transcriptional and chromatin genes disrupted in autism. Nature. 2014; 515:209–215. [PubMed: 25363760]

del Amo EM, Urtti A, Yliperttula M. Pharmacokinetic role of L-type amino acid transporters LAT1 and LAT2. European journal of pharmaceutical sciences : official journal of the European Federation for Pharmaceutical Sciences. 2008; 35:161–174. [PubMed: 18656534]

Folstein S, Rutter M. Genetic influences and infantile autism. Nature. 1977; 265:726–728. [PubMed: 558516]

Fotiadis D, Kanai Y, Palacin M. The SLC3 and SLC7 families of amino acid transporters. Molecular aspects of medicine. 2013; 34:139–158. [PubMed: 23506863]

Geier EG, Schlessinger A, Fan H, Gable JE, Irwin JJ, Sali A, Giacomini KM. Structure-based ligand discovery for the Large-neutral Amino Acid Transporter 1, LAT-1. Proceedings of the National Academy of Sciences of the United States of America. 2013; 110:5480–5485. [PubMed: 23509259]

Gkogkas CG, Khoutorsky A, Ran I, Rampakakis E, Nevarko T, Weatherill DB, Vasuta C, Yee S, Truitt M, Dallaire P, et al. Autism-related deficits via dysregulated eIF4E-dependent translational control. Nature. 2013; 493:371–377. [PubMed: 23172145]

Green TA, Alibhai IN, Unterberg S, Neve RL, Ghose S, Tamminga CA, Nestler EJ. Induction of activating transcription factors (ATFs) ATF2, ATF3, and ATF4 in the nucleus accumbens and their regulation of emotional behavior. The Journal of neuroscience : the official journal of the Society for Neuroscience. 2008; 28:2025–2032. [PubMed: 18305237]

Kilberg MS, Shan J, Su N. ATF4-dependent transcription mediates signaling of amino acid limitation. Trends in endocrinology and metabolism: TEM. 2009; 20:436–443. [PubMed: 19800252]

Kisanuki YY, Hammer RE, Miyazaki J, Williams SC, Richardson JA, Yanagisawa M. Tie2-Cre transgenic mice: a new model for endothelial cell-lineage analysis in vivo. Developmental biology. 2001; 230:230–242. [PubMed: 11161575]

Lam WK, Cleary MA, Wraith JE, Walter JH. Histidinaemia: a benign metabolic disorder. Archives of disease in childhood. 1996; 74:343–346. [PubMed: 8669938]

Lefauconnier JM, Trouve R. Developmental changes in the pattern of amino acid transport at the blood-brain barrier in rats. Brain research. 1983; 282:175–182. [PubMed: 6831239]

Mastroberardino L, Spindler B, Pfeiffer R, Skelly PJ, Loffing J, Shoemaker CB, Verrey F. Amino-acid transport by heterodimers of 4F2hc/CD98 and members of a permease family. Nature. 1998; 395:288–291. [PubMed: 9751058]

Menkes JH, Hurst PL, Craig JM. A new syndrome: progressive familial infantile cerebral dysfunction associated with an unusual urinary substance. Pediatrics. 1954; 14:462–467. [PubMed: 13214961]

Napolitano L, Scalise M, Galluccio M, Pochini L, Albanese LM, Indiveri C. LAT1 is the transport competent unit of the LAT1/CD98 heterodimeric amino acid transporter. The international journal of biochemistry & cell biology. 2015; 67:25–33. [PubMed: 26256001]

Novarino G, El-Fishawy P, Kayserili H, Meguid NA, Scott EM, Schroth J, Silhavy JL, Kara M, Khalil RO, Ben-Omran T, et al. Mutations in BCKD-kinase Lead to a Potentially Treatable Form of Autism with Epilepsy. Science. 2012

Romano E, Michetti C, Caruso A, Laviola G, Scattoni ML. Characterization of neonatal vocal and motor repertoire of reelin mutant mice. PloS one. 2013; 8:e64407. [PubMed: 23700474]

Santini E, Huynh TN, MacAskill AF, Carter AG, Pierre P, Ruggero D, Kaphzan H, Klann E. Exaggerated translation causes synaptic and behavioural aberrations associated with autism. Nature. 2013; 493:411–415. [PubMed: 23263185]

Sinclair LV, Rolf J, Emslie E, Shi YB, Taylor PM, Cantrell DA. Control of amino-acid transport by antigen receptors coordinates the metabolic reprogramming essential for T cell differentiation. Nature immunology. 2013; 14:500–508. [PubMed: 23525088]

Snyderman SE, Norton PM, Roitman E, Holt LE Jr. Maple Syrup Urine Disease, with Particular Reference to Dietotherapy. Pediatrics. 1964; 34:454–472. [PubMed: 14212461]

Trinh MA, Kaphzan H, Wek RC, Pierre P, Cavener DR, Klann E. Brain-specific disruption of the eIF2alpha kinase PERK decreases ATF4 expression and impairs behavioral flexibility. Cell reports. 2012; 1:676–688. [PubMed: 22813743]

Varoqueaux F, Jamain S, Brose N. Neuroligin 2 is exclusively localized to inhibitory synapses. European journal of cell biology. 2004; 83:449–456. [PubMed: 15540461]

Verrey F. System L: heteromeric exchangers of large, neutral amino acids involved in directional transport. Pflugers Arch. 2003; 445:529–533. [PubMed: 12634921]

Watson RE, Desesso JM, Hurtt ME, Cappon GD. Postnatal growth and morphological development of the brain: a species comparison. Birth defects research Part B, Developmental and reproductive toxicology. 2006; 77:471–484. [PubMed: 17066419]

Wolfson RL, Chantranupong L, Saxton RA, Shen K, Scaria SM, Cantor JR, Sabatini DM. Sestrin2 is a leucine sensor for the mTORC1 pathway. Science. 2016; 351:43–48. [PubMed: 26449471]

Yizhar O, Fenno LE, Prigge M, Schneider F, Davidson TJ, O'Shea DJ, Sohal VS, Goshen I, Finkelstein J, Paz JT, et al. Neocortical excitation/inhibition balance in information processing and social dysfunction. Nature. 2011; 477:171–178. [PubMed: 21796121]

Zeisel A, Munoz-Manchado AB, Codeluppi S, Lonnerberg P, La Manno G, Jureus A, Marques S, Munguba H, He L, Betsholtz C, et al. Brain structure. Cell types in the mouse cortex and hippocampus revealed by single-cell RNA-seq. Science. 2015; 347:1138–1142. [PubMed: 25700174]

Zinnanti WJ, Lazovic J, Griffin K, Skvorak KJ, Paul HS, Homanics GE, Bewley MC, Cheng KC, Lanoue KF, Flanagan JM. Dual mechanism of brain injury and novel treatment strategy in maple syrup urine disease. Brain. 2009; 132:903–918. [PubMed: 19293241]

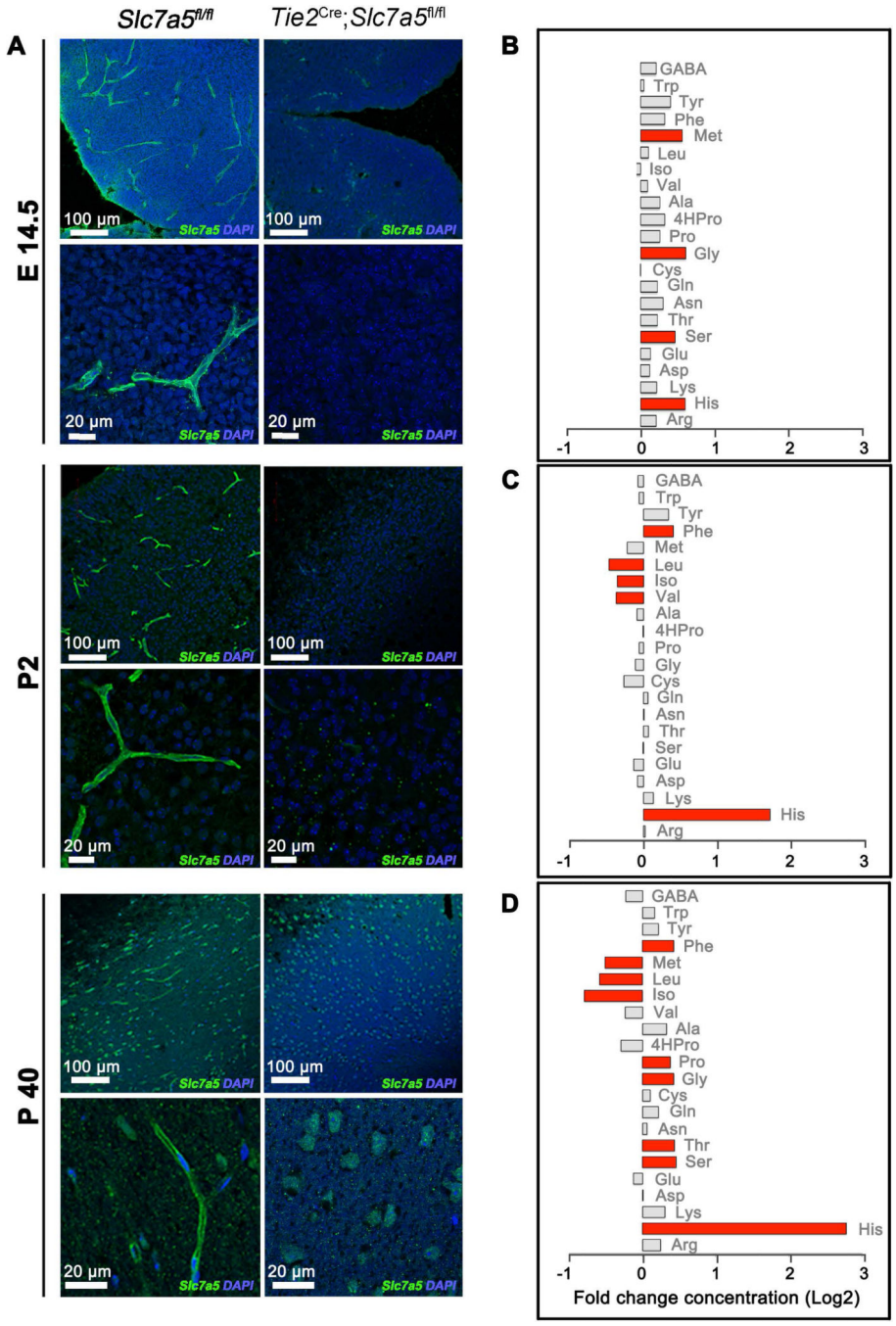

Figure 1. Slc7a5 mediates BCAA flux at the BBB

(A) Representative images showing Slc7a5 (green) localization at the BBB in control animals (*Slc7a5*$^{fl/fl}$, left) and its complete deletion in endothelial cells of the BBB in Cre positive mice (*Tie2*^{Cre}*;Slc7a5*$^{fl/fl}$, right). Immunostainings were performed in cortical slices at embryonic day 14.5 (E14.5 top), postnatal day 2 (P2, middle) and adulthood (>P40, bottom). Nuclei were stained with DAPI (blue). (B–D) Brain amino acid levels in *Tie2*^{Cre}*;Slc7a5*$^{fl/fl}$ mice at E14.5 (B), P2-14 (C) and >P40 (D). Levels of amino acids were normalized on protein concentration and shown as fold change (log2 transformed) to levels

in age-matched controls. In red are represented the amino acids with a fold change >1.3 and P value <0.05 (n>4 mice/genotype/time point).
See also Figure S1, S2 and Table S1.

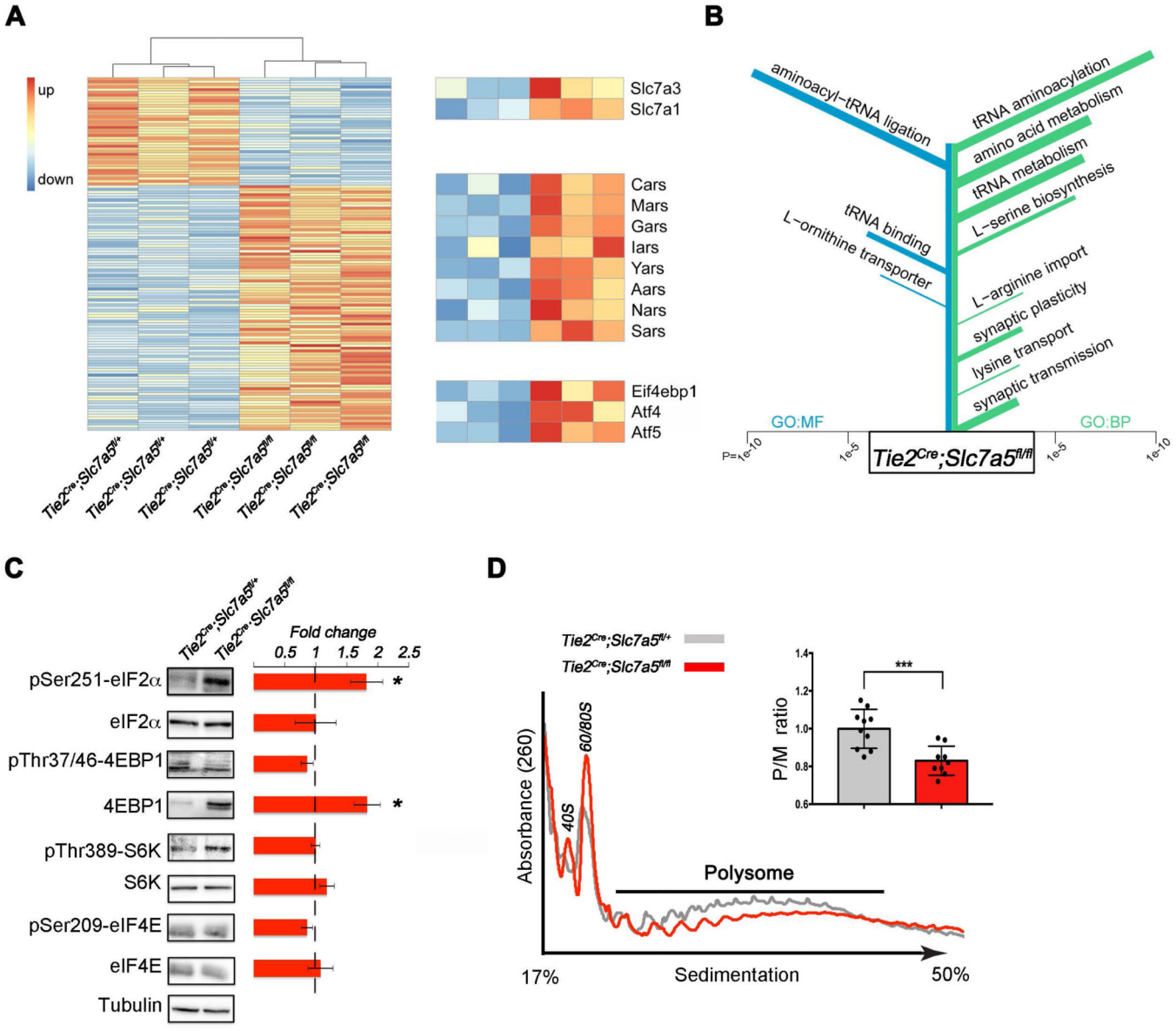

Figure 2. Activation of the amino acid response pathway in the brain of *Slc7a5* mutant mice

(A) RNA sequencing of adult brain in *Tie2*^{Cre};*Slc7a5*$^{fl/+}$ and *Tie2*^{Cre};*Slc7a5*$^{fl/fl}$ mice revealed 131 differentially expressed genes (FDR-adjusted P-value ≤ 0.05). The heat map displays log transformed count data normalized to library size. Genes expressed at lower levels in *Tie2*^{Cre};*Slc7a5*$^{fl/fl}$ (40 genes) are displayed at the top and genes up-regulated in *Tie2*^{Cre};*Slc7a5*$^{fl/fl}$ (91 genes) are shown at the bottom. Zoomed rows on the right emphasize differentially expressed genes associated with amino acid import (GO:0089718), tRNA aminoacylation (GO:0006418) and amino acid response, respectively (n=3 mice/genotype). (B) Results of GO Enrichment analysis on the set of 131 differentially expressed genes. Terms are sorted according to P-value with the most significantly enriched terms at the top: GO terms for molecular functions (GO:MF, left, blue); GO terms for biological processes (GO:BP, right, green). The length of each bar indicates the P-value while the width indicates the amount of genes in the set associated with the term.

(C) Western blot analysis from cortical lysates of *Tie2*^{Cre};*Slc7a5*$^{fl/+}$ (control) and *Tie2*^{Cre};*Slc7a5*$^{fl/fl}$ mice, indicating that mutants exhibit increased phospho-eIF2α and total 4EBP1 protein levels but normal levels of total eIF2α, phospho-4EBP1, phospho-S6K, S6K, phospho-eIF4E and eIF4E. Tubulin was used as internal control. Representative blots (left) and fold change ratio (right); *P<0.05 (means ± SEM; $n \geq 4$ mice/genotype).
(D) Polysome profile from cortical lysates of control and *Tie2*^{Cre};*Slc7a5*$^{fl/fl}$ mice. Typical tracings indicating positions of 40S, 60S and 80S ribosome peaks and polysome (P)/ monosome (M) ratio quantifications; ***P<0.001 (right inset: means ± SEM; $n=10$ control and $n=9$ mutant mice).

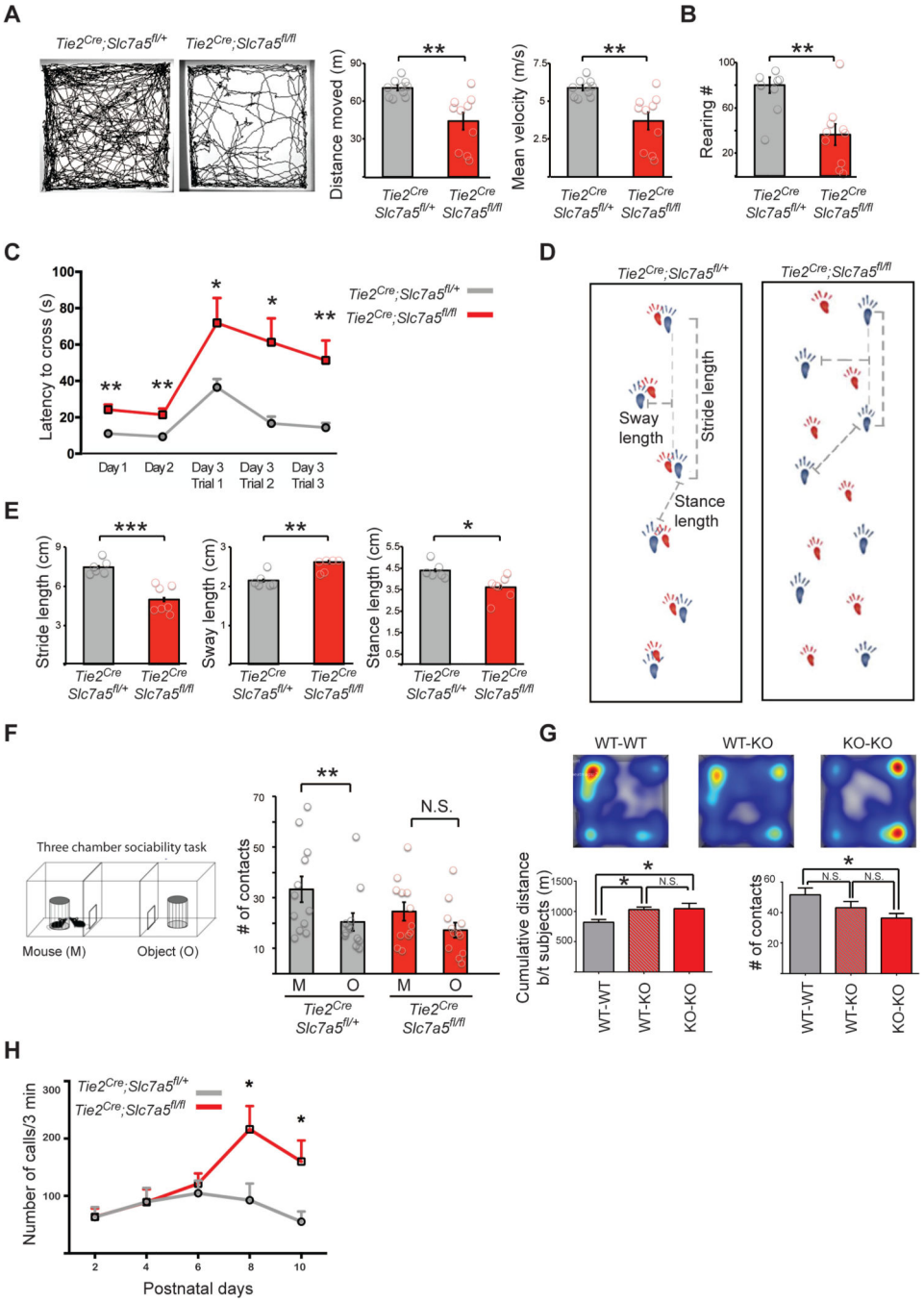

Figure 3. Neurobehavioral abnormalities in the *Tie2^{Cre};Slc7a5$^{fl/fl}$* mice

(A–D) Decreased exploratory behavior and locomotion abnormalities in the *Tie2^{Cre};Slc7a5$^{fl/fl}$* mice. (A) Open field test. Representative trajectories (left) and quantification of the total distance moved (middle) and the velocity (right) indicating that *Tie2^{Cre};Slc7a5$^{fl/fl}$* mice are outperformed by controls; **P<0.01 (means ± SEM; *n*=10 mice/genotype). (B) Comparison of the number of rearings pointing out deficiencies in the mutants; **P<0.01 (means ± SEM; *n*=10 mice/genotype) (C) Walking beam performance on training days (Day 1, Day 2) and on the three trials of the test day (Day 3), showing elevated

latency to cross the beam in the mutants; *P<0.05, **P<0.01 (means ± SEM; *n*=7 mice/genotype). (D) Representative images of control (left) and *Tie2*^{Cre};*Slc7a5*$^{fl/fl}$ strides (right) in the gait test. Forepaw (red) and hindpaw (blue). (E) Altered gait of the *Tie2*^{Cre};*Slc7a5*$^{fl/fl}$ mice is evidenced by inter-genotype comparison of stride, sway and stance length quantifications; *P<0.05, **P<0.01, ***P<0.001 (means ± SEM; *n*=7 mice/genotype). (F) Three chamber social interaction test (left) and quantifications (right) of the number of contacts with the caged mouse (M) or with the caged object (O) revealing abnormal social interaction pattern in the mutant mice (mutants show no preference for the M over the O, as opposed to controls); **P<0.01, N.S. not significant (means ± SEM; *n*=12 mice/genotype). (G) Juvenile *Tie2*^{Cre};*Slc7a5*$^{fl/fl}$ mice display fewer reciprocal social interactions. *Slc7a5* mutant mice tend to stay farther apart from their cage mate (heat-map and bottom left graph) and exhibit fewer nose-to-nose contacts (bottom right graph). WT= *Slc7a5*$^{fl/+}$; KO= *Tie2*^{Cre};*Slc7a5*$^{fl/fl}$. *P<0.05 (means ± SEM; *n*=8 mice/genotype). (H) Isolation induced USV at various postnatal days show that *Tie2*^{Cre};*Slc7a5*$^{fl/fl}$ mice emit an increased number of calls starting at P8. *P<0.05 (means ± SEM; *n*=10 mice/genotype). See also Figure S3.

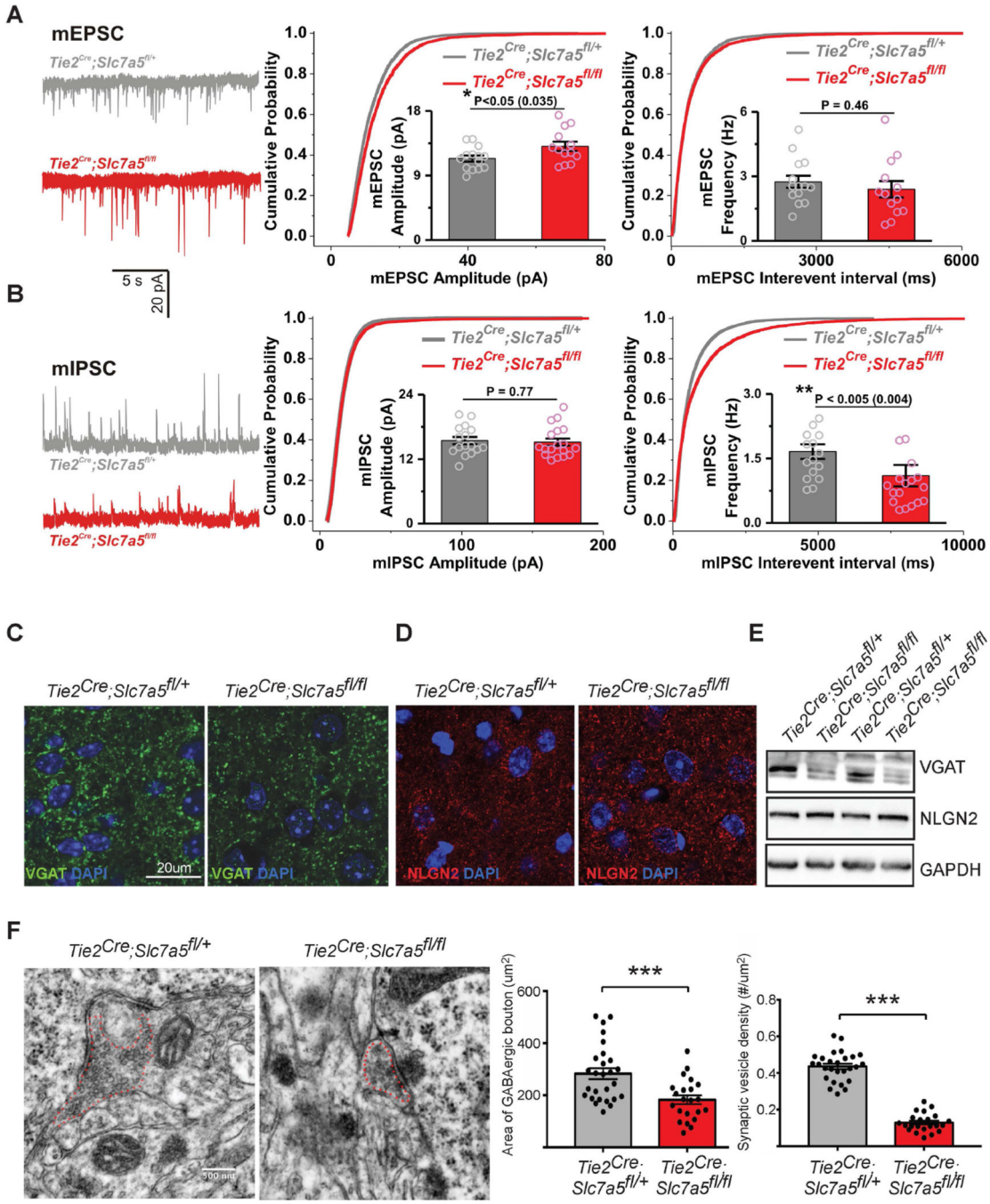

Figure 4. Excitation/inhibition imbalance in *Tie2^{Cre};Slc7a5$^{fl/fl}$* somatosensory cortex

(A–B) Left: Representative mEPSC (A) and mIPSC (B) recordings from *Tie2^{Cre};Slc7a5$^{fl/+}$* and *Tie2^{Cre};Slc7a5$^{fl/fl}$* somatosensory cortex (SCX) layers 2–3 pyramidal neurons; Right: Cumulative probability distributions of peak amplitudes and inter-event intervals of mEPSC (A) and mIPSC (B) in the two genotypes. Insets: quantifications of mean amplitudes and mean frequencies of the corresponding currents, with significant differences in mutants versus controls. D=0.093, P<10^{-11} (mEPSC amplitudes) and D=0.099, P<10^{-15} (mIPSC interevent intervals); (means ± SEM, $n_{cells}/n_{animals}$/genotype: 14/7/*Tie2^{Cre};Slc7a5$^{fl/+}$* and

13/5/*Tie2^{Cre};Slc7a5$^{fl/fl}$* (mEPSC); 16/7/*Tie2^{Cre};Slc7a5$^{fl/+}$* and 18/5/*Tie2^{Cre};Slc7a5$^{fl/fl}$* (mIPSC).

(C) Representative confocal images of VGAT-positive synaptic puncta (green) in control (left) and *Tie2^{Cre};Slc7a5$^{fl/fl}$* (right) cortical sections displaying decreased staining intensity in the mutants. Nuclei were stained with DAPI (blue).

(D) Confocal imaging of cortical sections labeled for Neuroligin 2 (NLGN2, red) of control (left) and *Tie2^{Cre};Slc7a5$^{fl/fl}$* (right) animals revealing no difference between genotypes. Nuclei were stained with DAPI (blue). Scale bar as in (C).

(E) Western blot analysis from cortical lysates indicating decreased VGAT (top) and similar NLGN2 protein levels (middle) in *Tie2^{Cre};Slc7a5$^{fl/fl}$* mice compared with controls. GAPDH (bottom) was used as internal control.

(F) Electron microscopy imaging of the SCX layers 2–3 showing that *Tie2^{Cre};Slc7a5$^{fl/fl}$* mice have a decreased area of GABAergic boutons and decreased density of vesicles per bouton. Typical micrograph images (left), summary graphs of presynaptic area (middle) and vesicle density (right); ***P<0.001 (means ± SEM; $n_{synapses}$/genotype: 27/control and 22/mutant).

See also Figure S4 and S5.

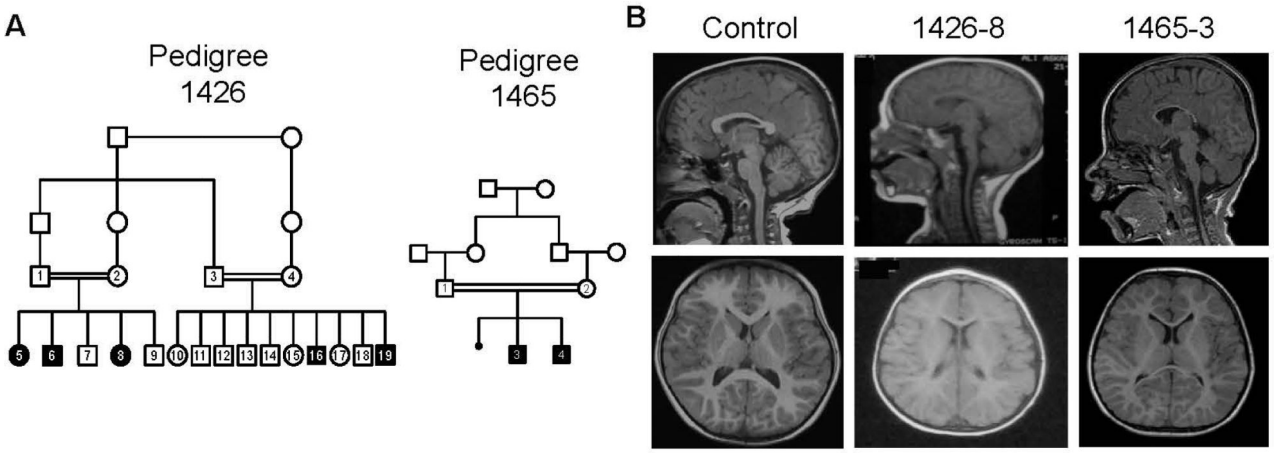

C

Patient	1426-5	1426-6	1426-8	1426-19	1465-3	1465-4
Gender	F	M	F	M	M	M
Origin	Libya	Libya	Libya	Libya	Turkish	Turkish
Age at diagnosis	N/A	N/A	5 months	N/A	2 weeks	5-6 months
HC at birth (SD)	N/A	-2/-3	N/A	N/A	- 3	- 3
HC at latest examination (SD)	-5	-2,3	-5,5	-5	N/A	N/A
Developmental milestones						
Gross motor (normal/delayed/absent)	Delayed	Delayed	Delayed	Delayed	Delayed	Delayed
Fine motor (normal/delayed/absent)	Delayed	Delayed	Delayed	Delayed	Delayed	Delayed
Language (normal/delayed/absent)	Delayed	Delayed	Delayed	Delayed	Absent	Absent
Social (normal/delayed/absent)	Delayed	Delayed	Delayed	Delayed	Delayed	Delayed
Seizure						
Type	-	-	-	N/A	GTC	GTC
Onset	-	-	-	N/A	1year	6 months
Autism associated disorder						
Impaired social interactions	+	+	+	N/A	+	+
Impaired eye-to-eye gaze, facial expression	+	+	+	N/A	+	+
Impaired ability to form peer relationships	+	+	+	N/A	+	+
Lack of spontaneous play	+	+	+	N/A	+	+
Restrictive behavior, interests and activities	+	+	+	N/A	+	+
Stereotyped, repetitive behavior	-	-	-	N/A	+	+
Inflexible adherence to routines or rituals	+	+	+	N/A	+	+
Additional CNS investigations						
MRI	N/A	Cortical atrophy	Normal	N/A	Thin CC	Thin CC

Figure 5. Mutations in the human *SLC7A5* lead to ASD and motor deficits

(A) *SLC7A5* mutations identified in families 1426 and 1465 in individuals with ASD, motor deficits and microcephaly. Pedigrees 1426 and 1465 display first-cousin consanguinity, five and two affected patients (solid symbols) respectively and unaffected members (open symbols)

(B) MRI from one patient for each family showing microcephaly and thin corpus callosum but normal axial T1 sequence of the brain. Control child brain MRIs were obtained from unrelated individuals.

(C) Clinical presentation of patients from family 1426 and 1465. HC, head circumference; SD, standard deviation; GTC, generalized tonic clonic; N/A not available; CC, corpus callosum.

See also Table S2.

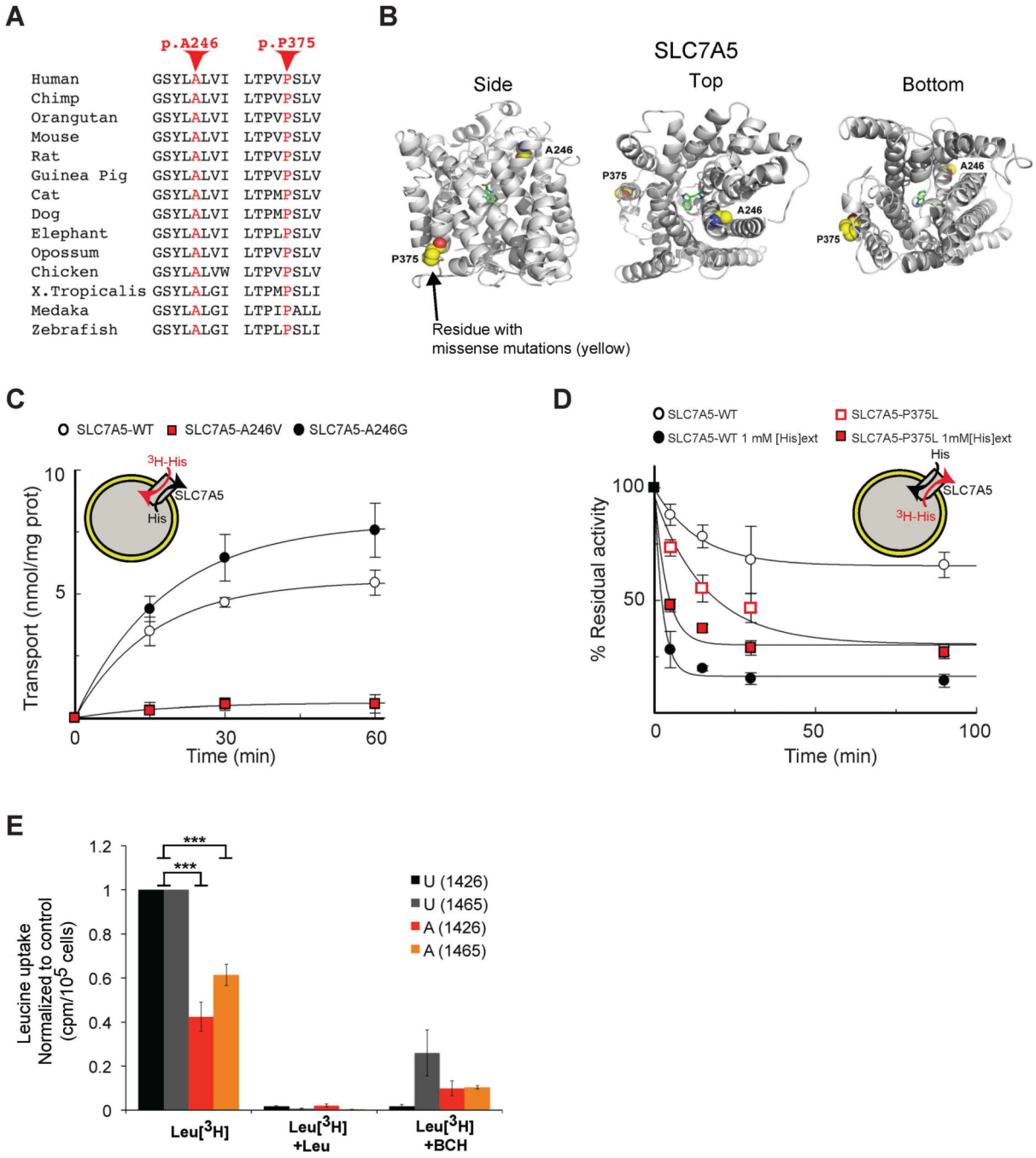

Figure 6. A246V and P375L mutations compromise SLC7A5 function

(A) Conservation of the SLC7A5 A246 and P375 in several species.

(B) Side, top and bottom views of the predicted structure of SLC7A5 in complex with tryptophan showing SLC7A5 backbone atoms (gray ribbon), atoms of the residues constituting the missense mutations (yellow spheres) and the ligand tryptophan (green sticks); oxygen atoms (red) and nitrogen atoms (blue).

(C) SLC7A5 wild-type, A246V and A246G mutants over-expressed and purified by fast protein liquid chromatography were reconstituted in proteoliposomes. Transport is followed

as uptake (red arrow) of external [^{3}H]His in exchange with internal His. Transport was started by adding external 5 μM [^{3}H]His at time zero to proteoliposomes containing 10 mM His reconstituted with SLC7A5-WT (○), SLC7A5-A246V (■) or SLC7A5-A246G (●) and stopped at the indicated times (means ± SD; n=5 experiments).

(D) Time dependence of [^{3}H]His efflux from proteoliposomes reconstituted with SLC7A5-WT or SLC7A5-P375L was measured. Proteoliposomes reconstituted with SLC7A5-WT (○, ●) or SLC7A5-P375L (□, ■), containing 2 mM His were radioactivity-preloaded. Efflux was measured in absence (○, □; uniport) or presence of external 1 mM His (●, ■; antiport). Percentage of His efflux was calculated with respect to time 0 (means ± SD; n=4 experiments).

(E) Radio-labeled leucine ([^{3}H]Leu) transport analysis in human fibroblasts from affected (A) and unaffected (U) members of families 1426 and 1465 illustrating a significant reduction in leucine uptake by the cells of affected patients. Specificity of leucine uptake was assessed by competition with 10mM cold leucine (Leu) or 10 mM 2 BCH; ***P<0.001 (means ± SEM; N≥3 experiments performed with fibroblasts from two patients and one healthy control/family).

See also Figure S7.

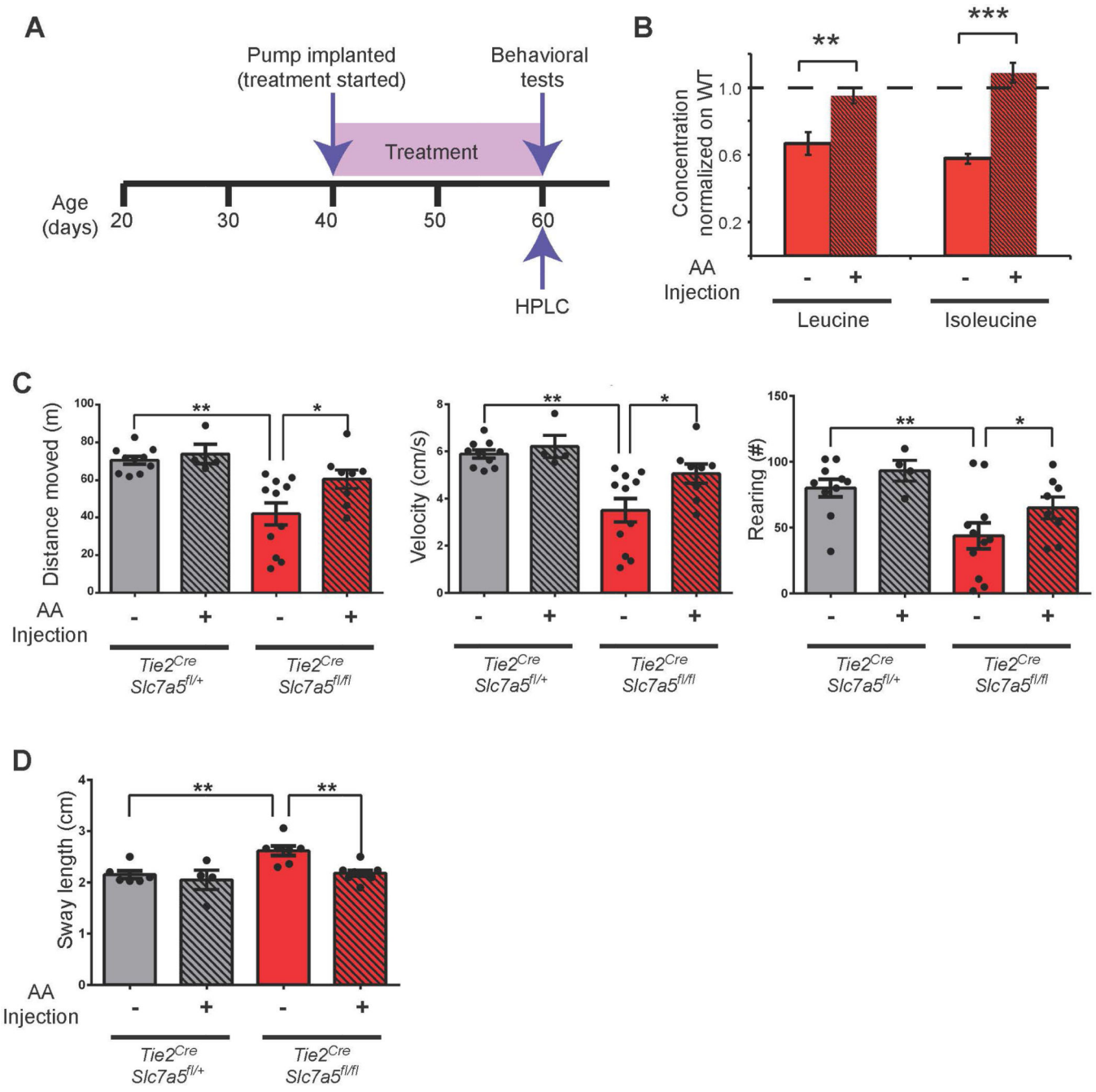

Figure 7. Normalization of *Tie2*^{Cre};*Slc7a5*$^{fl/fl}$ mouse behavior after leucine and isoleucine i.c.v. administration

(A) Timeline of treatment and HPLC and behavioral tests.

(B) Brain levels of leucine (left) and isoleucine (right) in age-matched animals receiving (+) or not receiving (−) the i.c.v. treatment. Amino acid levels were normalized to protein concentration and to wild-type levels. **P<0.01, ***P<0.001 (means ± SEM; *n*=8 mice/genotype).

(C) Quantification of the total distance moved (left), velocity (middle) and number of rearings (right) in the open field revealing similar behavior in treated (+) *Tie2*^{Cre};*Slc7a5*$^{fl/fl}$

mice and non-treated (−) or treated (+) controls (*Tie2*^{Cre};*Slc7a5*$^{fl/+}$) but significant differences with non-treated (−) *Tie2*^{Cre};*Slc7a5*$^{fl/fl}$ mice; *P<0.05, **P<0.01 (means ± SEM; *n*=10 (−) control, *n*=4 (+) control, *n*=11 (−) mutant and *n*=8 (+) mutant).

(D) Similar sway length in treated (+) mutant mice and non-treated (−) or treated (+) control (*Tie2*^{Cre};*Slc7a5*$^{fl/+}$) animals but significant difference with non-treated (−) *Tie2*^{Cre};*Slc7a5*$^{fl/fl}$ mice; **P<0.01 (means ± SEM; *n*=10 (−) control, *n*=4 (+) control, *n*=11 (−) mutant and *n*=8 (+) mutant).

See also Table S3.